Inviscid Damping of Elliptical Perturbations on a 2D Vortex

D.A. Schecter, D.H.E. Dubin, A.C. Cass
C.F. Driscoll, I.M. Lansky and T.M. O'Neil

Physics Department
University of California at San Diego, La Jolla, CA 92093

Abstract. The inviscid damping of an elliptical perturbation on a 2D vortex is examined experimentally and theoretically. The perturbation is generated by an impulse at the wall. Initially, the quadrupole moment (ellipticity) of the perturbation decays exponentially. This result is significant, since arbitrary perturbations need not decay exponentially. The decay rate is given by a "Landau pole" of the equilibrium profile. When the Landau damping is weak, the vorticity perturbation, in addition to the quadrupole moment, behaves like an exponentially damped mode. This "quasi-mode" is actually a wave-packet of exceptional continuum modes that decays as the continuum modes disperse.

The inviscid relaxation of a 2D vortex after a weak external impulse is studied experimentally and theoretically. In the experiments, the 2D fluid is a strongly magnetized electron plasma in a cylindrical Penning trap, with wall radius R_w [1,2]. These electron plasmas have negligible viscosity and are governed approximately by the 2D Euler equations:

$$\partial\zeta/\partial t + \vec{v}\cdot\nabla\zeta = 0, \qquad \vec{v} = \hat{z}\times\nabla\psi, \qquad \text{and} \quad \nabla^2\psi = \zeta. \tag{1}$$

Here, $\vec{v}(r,\theta,t)$ is the ($\mathbf{E}\times\mathbf{B}$ drift) velocity field in the plane perpendicular to the trap-axis, $\zeta(r,\theta,t) \equiv \hat{z}\cdot\nabla\times\vec{v}$ is the vorticity, and $\psi(r,\theta,t)$ is a stream function. The boundary condition is $\psi = 0$ at R_w.

EXPERIMENTS

Figure 1 shows two experiments that illustrate the process of "inviscid damping" [2–8]. In both experiments, we excite an elliptical ($m = 2$) perturbation on an initially circular vortex. The initial vorticity distribution $\zeta_o(r)$ and the initial rotation frequency $\Omega_o(r)$ are monotonically decreasing functions of radius, making the vortex stable [4]. In experiment (a), the impulse excites an undamped elliptical mode, with frequency ω. The fluid rotation is resonant with this mode at a radius

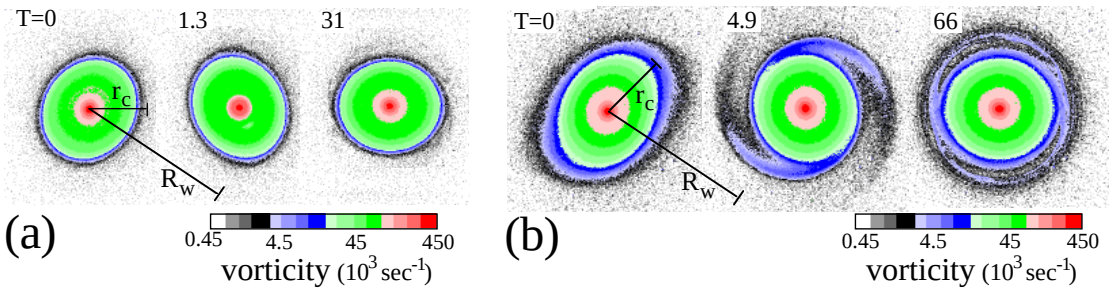

FIGURE 1. Experiments. **a)** An undamped mode is excited, with critical radius r_c outside the vortex. **b)** Inviscid damping occurs when r_c is inside the vortex. In both experiments, the unperturbed vorticity $\zeta_o(r)$ decreases monotonically with r. Time is measured in central rotation periods: $T \equiv t \cdot \Omega_o(0)/2\pi$.

r_c, defined by $2\Omega_o(r_c) = \omega$, and this critical radius lies outside the vortex. The vortex in (b) is similar to the vortex in (a), except that $\zeta_o(r)$ extends past the critical radius r_c. The excited mode is now damped by resonant mixing of vorticity at r_c. This inviscid damping is analogous to collisionless Landau damping, where a compressional plasma wave decays due to its interaction with charged particles that travel at the same velocity as the wave [4].

Figure 2 shows the evolution of the quadrupole moment Q_2 of the perturbation in Fig. 1(b). We define the quadrupole moment by the equation

$$Q_2 \equiv \int_0^{R_v} dr\ r^3 \delta\zeta^{(2)}(r,t), \tag{2}$$

where R_v is the vortex radius, and $\delta\zeta^{(2)}$ is the $m = 2$ Fourier component of the vorticity perturbation. The amplitude of Q_2 is a measure of ellipticity. Also plotted in Fig. 2 is the theoretical *linear* response of the vortex to an externally applied $\delta(t)$ impulse. Initially, there is good agreement between linear theory and the experiment. However, after 5 rotations, the experiment diverges from linear theory, and the amplitude of Q_2 begins to oscillate. These nonlinear oscillations are due to mixing of trapped vorticity at r_c. Eventually, the amplitude saturates, and the vortex relaxes to a rotating "cat's eyes" equilibrium [Fig. 1(b), far right].

For the remainder of this paper, we focus on the initial linear decay, which properly describes the evolution for arbitrarily long times if the amplitude is sufficiently small [2]. Figure 2 indicates that the initial decay of Q_2 is approximately exponential, i.e. $|Q_2(t)| \approx |Q_2(0)|e^{-\gamma t}$. This result is generic to the experiments, and is significant, since arbitrary linear perturbations need not decay exponentially. Of equal interest is that, when the damping is weak ($\gamma/\omega << 1$), the actual vorticity perturbation behaves like an exponentially damped eigenmode: $\delta\zeta(r,t) \approx \xi(r)e^{-\gamma t}e^{-i\omega t}$, for $r \lesssim r_c$. This perturbation is referred to as a "quasi-mode", since it is not an exact eigenmode of the Euler equations.

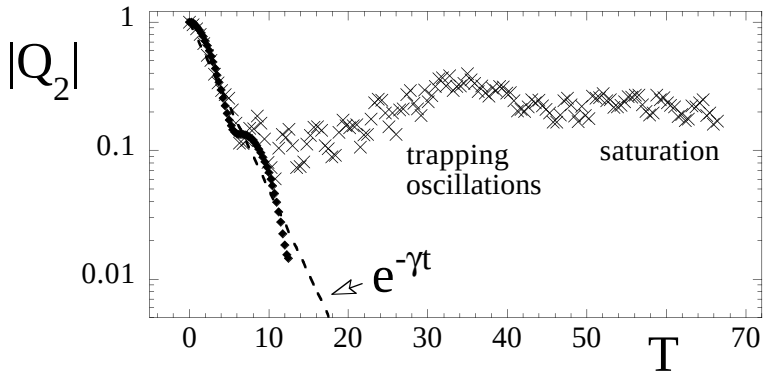

FIGURE 2. Typical evolution of the quadrupole moment, Q_2. The X's give Q_2 for the experiment in Fig. 1(b). The diamonds correspond to linear theory. The dashed line is an exponential fit to the initial decay.

LINEAR EIGENMODE THEORY

As pointed out by Case [9], a linear vorticity perturbation varying as $e^{im\theta}$ can be viewed as a sum of discrete modes plus an integral of continuum modes (also called "shear-waves") [9–11]:

$$\delta\zeta(r,t) = \sum_d A(\omega_d)\xi_d(r)e^{-i\omega_d t} + \int d\omega A(\omega)\xi_\omega(r)e^{-i\omega t} \tag{3}$$

We will use the index k to refer to both discrete and continuum modes. These eigenmodes satisfy the following integral eigenvalue equation:

$$m\Omega_o(r)\xi_k(r) - \frac{m}{r}\zeta_o'(r)\int_0^{R_v} dr' r' G_m(r|r')\xi_k(r') \;=\; \omega_k\xi_k(r), \tag{4}$$

where ζ_o' is the radial derivative of the equilibrium vorticity. The Green's function in Eq. (4) is given by $G_m(r|r') = -\frac{1}{2m}\left(\frac{r_<}{r_>}\right)^m\left[1-\left(\frac{r_>}{R_w}\right)^{2\mathrm{m}}\right]$. Here, $r_>$ ($r_<$) is the greater (smaller) of r and r'.

The eigenmodes can be obtained numerically by discretizing Eq. (4) in r. This leads to a standard matrix eigenvalue equation, $\sum_j M_{ij}\xi_k(r_j) = \omega_k\xi_k(r_i)$. If there are N radial grid-points between 0 and R_v, then a solution to the matrix equation gives N eigenmodes. Any linear initial value problem can be solved numerically with a superposition of these eigenmodes: $\delta\zeta(r,t) \approx \sum_{k=1}^{N} A(\omega_k)\xi_k(r)e^{-i\omega_k t}$. The solution generally breaks down for times greater than the minimum value of $2\pi/m\Omega_o'\Delta r$, where Δr is the radial grid-point spacing and $\Omega_o'(r)$ is the radial derivative of the rotation frequency.

When there are no discrete modes, the perturbation consists entirely of continuum modes. It is common (but often misleading) to view this perturbation intuitively as a passive scalar in the equilibrium shear flow. However, a quasi-mode is a superposition of continuum modes that does not behave like a passive scalar.

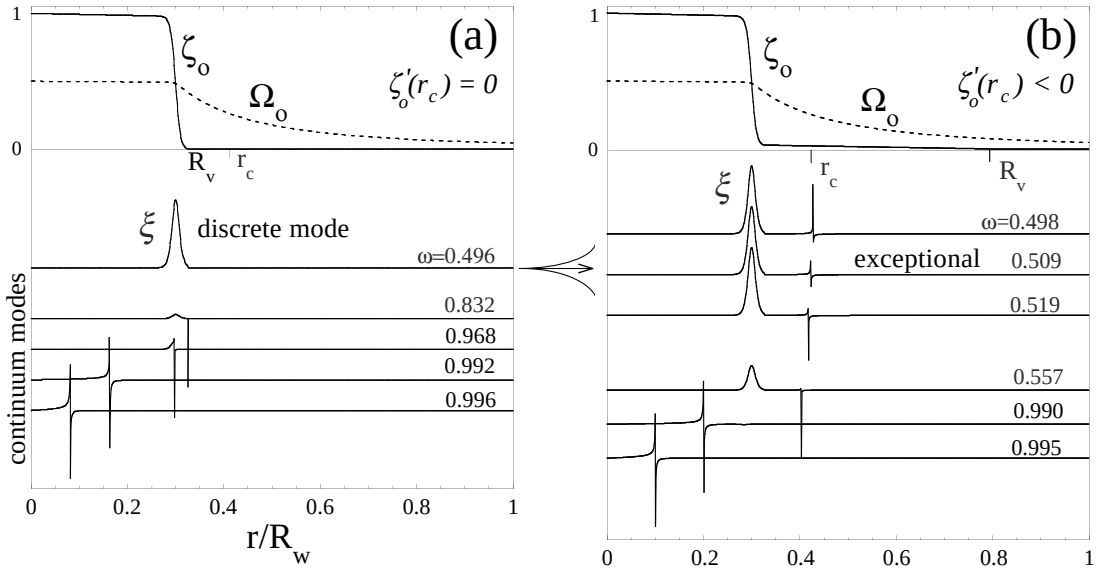

FIGURE 3. Equilibrium profiles and ($m = 2$) radial eigenfunctions for a top-hat vortex with a discrete mode (a), and a top-hat vortex with a quasi-mode (b).

One goal of this paper is to clarify how the "phase-mixing" of continuum modes is consistent with the observed quasi-modes.

It is useful to compare a quasi-mode, which exists when $\zeta_o'(r_c) < 0$, to an undamped discrete mode, which exists when $\zeta_o'(r_c) = 0$. Figure 3(a) shows the $m = 2$ eigenmodes of a "top-hat" vortex, similar to that studied by Kelvin [12]. This top-hat supports a single discrete mode, which has a critical radius $r_c > R_v$, and a set of continuum modes that have eigenfrequencies in the range $2\Omega_o(R_v) < \omega_k < 2\Omega_o(0)$. Figure 3(b) shows the eigenmodes of a similar vortex, with a skirt of vorticity that tapers past r_c. The negative vorticity gradient at r_c causes the discrete mode to be replaced by a wave-packet of continuum modes. The continuum modes in this wave-packet are labelled "exceptional" in Fig. 3(b), since they are approximately the same as the original discrete mode. The only noticeable difference is that each continuum mode has a singular spike near r_c, where the fluid rotation is resonant with the mode. As we will soon see, the wave-packet that replaces the undamped discrete mode evolves as a quasi-mode, which decays exponentially (at early times) as the continuum modes disperse.

LINEAR RESPONSE TO AN IMPULSE

We now consider the response of the vortices in Fig. 3 to a brief external impulse, of strength ε. The impulse is applied at the wall, and creates an instantaneous "external" stream function, $\psi_{ext}(r, \theta, t) = \varepsilon\delta(t)(r/R_w)^2 e^{i2\theta}$. A straight-forward

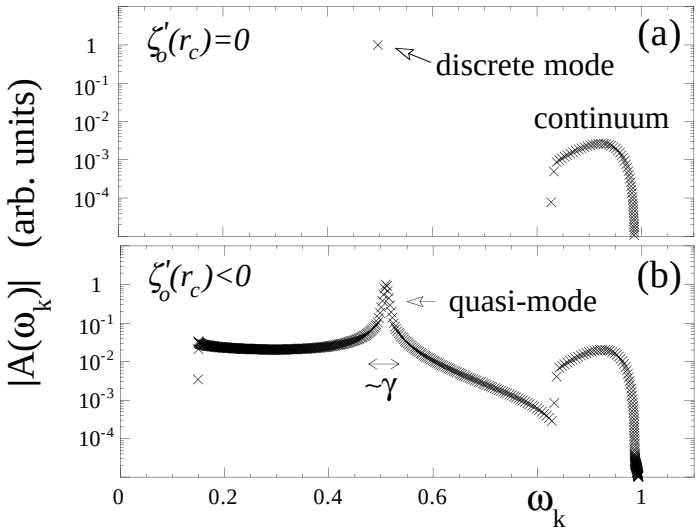

FIGURE 4. The ($m = 2$) eigenmode amplitudes after an impulse is applied to a top-hat vortex with a discrete mode (a), and a top-hat vortex with a quasi-mode (b).

calculation shows that, for a monotonic vortex, the complex amplitude of each eigenmode (immediately) after the impulse is given by

$$A(\omega_k) = i\frac{2\varepsilon}{(R_w)^2}\frac{\langle \xi_k, r\zeta_o' \rangle}{\langle \xi_k, \xi_k \rangle} = -i\frac{2\varepsilon}{(R_w)^2}\frac{\int_0^{R_v} dr\ r^3 \xi_k(r)}{\langle \xi_k, \xi_k \rangle}. \tag{5}$$

Here, $\langle f, h \rangle$ is short-hand for the inner-product $\int_0^{R_v} dr\ r^2 f^*(r)h(r)/|\zeta_o'(r)|$. Equation (5) indicates that the excitation of an eigenmode is proportional to its (scaled) multipole moment (here the quadrupole moment, since $m = 2$). In this sense, the system exhibits reciprocity: the eigenmodes that produce the largest external fields are also the most sensitive to excitation by a brief external impulse.

Figure 4 shows the response of both vortices in Fig. 3 to an external impulse. In case (a), the discrete mode is excited about 100 times more strongly than any of the continuum modes. In case (b), a similar initial perturbation is excited, but it now decomposes into a sharply peaked distribution of continuum modes. The continuum modes in the peak region are exceptional, in that they are similar in form to the original discrete mode (see Fig. 3). Due to this similarity, and the sharply peaked distribution, the excitation will behave like an exponentially damped version of the original discrete mode. The decay rate γ of this quasi-mode is proportional to the width of the peak in $A(\omega_k)$. Note that the simple mode-like behavior of the excitation breaks down near r_c, where the continuum modes have singular spikes. Here, the perturbation forms filaments, like those seen in the experiments [Fig. 1(b)].

The evolution of the quadrupole moment of the excitation in case (b) is shown in Fig. 5. At early times, the amplitude of Q_2 decays exponentially. The inset shows that, for $r \lesssim r_c$, the vorticity perturbation merely decays as a damped

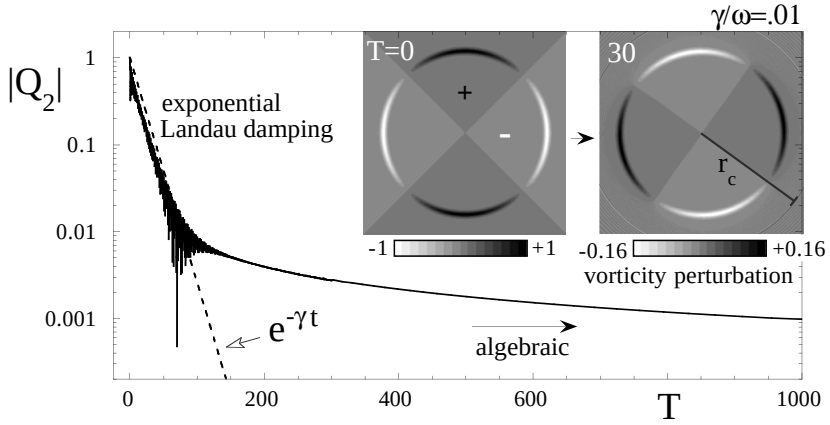

FIGURE 5. Evolution of an excited quasi-mode on a top-hat vortex [Fig. 3(b)]. The dashed line is exponential Landau damping, given by Eq. (6). The vorticity perturbation (inset) behaves like a damped, rotating mode (for $T \lesssim 100$ and $r \lesssim r_c$). The '+' and '−' signs indicate regions of positive and negative vorticity perturbation.

mode, without shearing apart. Near r_c, the perturbation actually grows to a finite amplitude and then filaments (not visible). Eventually, the decay of Q_2 turns algebraic, as it must for all linear perturbations on a stable vortex that has no discrete modes [4].

Exponential decay of Q_2 is apparently the "generic" evolution after an external impulse excitation. This is significant, since arbitrary perturbations can (and often do) evolve with no stage of exponential decay. However, the possibility of exponential decay has been known for some time. A general solution to the initial value problem shows that any perturbation will have a contribution from a "Landau pole" of the equilibrium profile [4–6]. This contribution behaves exactly like an exponentially damped mode, but never represents a complete solution to the initial value problem.

The Landau pole for the top-hat profile in Fig. 3(b) gives the following exponential decay rate [4]:

$$\gamma \approx -\frac{\pi}{8} r_o \zeta_o'(r_c) \left(\frac{r_o}{r_c}\right) \left[1 - \left(\frac{r_c}{R_w}\right)^4\right]^2 , \tag{6}$$

where r_o is the radius at which ζ_o' is maximal. Equation (6) is derived in Ref. [4], under the assumption that $\zeta_o'(r_c)$ is close to zero. The dashed line in Fig. 5 corresponds to exponential decay that is given solely by the Landau pole [Eq. (6)]. Clearly, the Landau pole gives the correct decay rate of an impulse generated perturbation on a top-hat vortex.

Figure 6 shows the response of a Gaussian vortex, $\zeta_o(r) = e^{-(5r/R_w)^2}$, to an external impulse. As before, the initial decay of Q_2 is exponential and dominated by the Landau pole. Here, the Landau pole was calculated numerically, using the method of Spencer and Rasband [6].

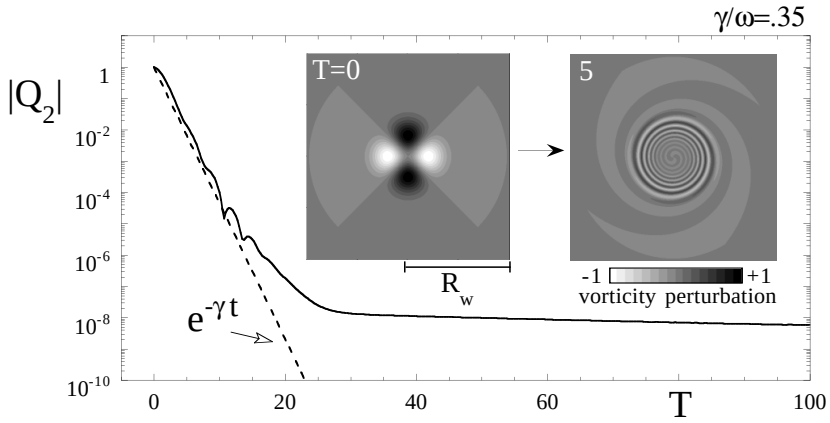

FIGURE 6. Decay of an impulse generated perturbation on a Gaussian vortex. The dashed line corresponds to the exponential decay that is given by a Landau pole, which is calculated numerically [6].

Although Q_2 decays exponentially, the vorticity perturbation (inset) does not behave like an exponentially damped mode. This is due to the large decay rate $\gamma/\omega = .35$, compared to the previous case where $\gamma/\omega = 0.01$. Because γ is large, the excitation has a broadly peaked distribution of continuum modes, with resonant radii (and singular spikes) spanning most of the vortex. The evolution of such perturbations is characterized by the "spiral wind-up" [13–15] that is observed here.

SUMMARY

In this paper, we examined the inviscid damping of elliptical perturbations on a 2D vortex. Specifically, we considered perturbations that were generated by an impulse, applied at the wall. It was shown that, in general, exponential Landau damping properly describes the initial decay of the perturbation's quadrupole moment Q_2, despite the fact that arbitrary perturbations need not decay exponentially. We also showed that when Landau damping is weak ($\gamma/\omega << 1$), the vorticity perturbation $\delta\zeta$ behaves like an exponentially damped mode (for $r \lesssim r_c$). This quasi-mode was identified as a wave-packet of exceptional continuum modes that decays exponentially as the continuum modes disperse. When Landau damping is strong ($\gamma/\omega \sim 1$), the vorticity perturbation exhibits spiral wind-up, and does not resemble a mode.

ACKNOWLEDGEMENT

This work was supported by the National Science Foundation (NSF PHY-9876999).

REFERENCES

1. C. F. Driscoll and K. S. Fine, Phys. Fluids B **2**, 1359 (1990);
2. S. Pillai and R.W. Gould, Phys. Rev. Lett. **73**, 2849 (1994).
3. M.V. Melander, J.C. McWilliams and N.J. Zabusky, J. Fluid Mech. **178**, 137 (1987).
4. R. J. Briggs, J. D. Daugherty, and R. H. Levy, Phys. Fluids **13**, 421 (1970).
5. N.R. Corngold, Phys. Plasmas **2**, 620 (1995).
6. R.L. Spencer and S.N. Rasband, Phys. Plasmas **4**, 53 (1997).
7. A.C. Cass, Ph.D. dissertation, University of California at San Diego (1998).
8. D.A. Bachman, Ph.D. dissertation, California Institute of Technology (1997).
9. K.M. Case, Phys. Fluids **3**, 143 (1960).
10. G.G. Sutyrin, Sov. Phys. Dokl. **34**, 104 (1989).
11. M.T. Montgomery and C. Lu, J. Atmos. Sci. **54**, 1868 (1997).
12. Lord Kelvin, Phil. Mag. **10**, 155 (1880).
13. A.J. Bernoff and J.F. Lingevitch, Phys. Fluids **6**, 3717 (1994).
14. A.P. Bassom and A.D. Gilbert, J. Fluid. Mech. **371**, 109 (1998).
15. P.B. Rhines and W.R. Young, J. Fluid Mech. **133**, 133 (1983).